Research Article   Open Access

Bismuth Mass Fraction Determination in Thin Films by an ICP-AES Validated Method and Uncertainty Estimation

Olfa Dachraoui[1], Atef Atyaoui[2*], Faouizi Manaii[2], Hager Maghraoui-Meherzi[1] and Chokri Loukil[2]

[1]University of Tunis El Manar, Faculty of Sciences of Tunis, LR99ES15 Laboratory of Analytical Chemistry and Electrochemistry, 2092, Tunis, Tunisia.

[2]Chemical Analysis Laboratory, National Offices of Mines of Tunisia, 24, rue de L'Energie, 2035 La Charguia - Tunis | BP: 215 - 1080 Tunis Cedex – Tunisia.

[*]**Corresponding Author:** Atef Atyaoui, Chemical Analysis Laboratory, National Offices of Mines of Tunisia, 24, rue de L'Energie, 2035 La Charguia - Tunis | BP: 215 - 1080 Tunis Cedex – Tunisia. E-mail address: atyaoui.atef@gmail.com.

Abstract

This paper covers the validation and measurement uncertainty evaluation of an ICP-AES method for bismuth mass fraction determination in bismuth sulfide thin films. Plasma view at radial mode and the wavelength were monitored for bismuth at 223.061 nm. Following AFNOR (Association Française de Normalisation) Norm NFT 90-210 (2009), a regression equation was calculated using single element bismuth standard solution prepared in the same matrix as samples. The linear range was between 0.2 and 2.0 mg L^{-1}. Limits of detection (LOD) and quantification (LOQ) were calculated as 0.03 and 0.12 mg L^{-1}, respectively. Recovery percentages were ranging between 91 and 109 %. Accuracy was found to be adequate. Estimated expanded uncertainty according to both GUM and EURACHEM guides was 3.1 %.

Keywords: validation; uncertainty estimation; bismuth; thin films; chemical bath deposition; ICP-AES.

Introduction

During the last three decades, a revival, as well as a rapid expansion in the research of semiconducting chalcogenides thin films, have been witnessed. Among them, binary semiconductors of $A^V B^{VI}$ type have been receiving attention due to their potential use in optoelectronic devices [1-4]. Bismuth sulfide belongs to this group whose interesting properties make it a good candidate for several applications such as liquid junction solar cells [5,6], photodetectors [7,8], electrochemical storage of hydrogen [9], and detection of biomolecules [10] and gas [11,12].

Inductively coupled plasma atomic emission spectrometry (ICP-AES) is a strong tool for the determination of multi-element mass fractions in liquid and solid samples [13], with sufficiently low detection limit, selectivity, speed, precision, and wide analytical (dynamic) range [14]. Various ICP-AES measurement methods exist in the literature for the determination of bismuth mass fractions in different matrices. Analysis of impurities in bismuth oxide has been conducted by this technique [15]. In addition, corrosion behavior properties of pure Pb, Sb, and Bi tellurides were investigated in a chloride environment using inductively coupled plasma atomic emission spectrometry associated with micro-Raman [16]. Besides, other (ICP-AES) methods have been used for the determination of bismuth in matrices such as biological and environmental samples [17,18], human urine [19], and natural water [20]. However, to the best of our knowledge, there is no validated measurement procedure for the analysis of bismuth on chalcogenides thin films.

The main objective of this study is to validate a suitable ICP-AES method to quantify bismuth in bismuth sulfide thin films prepared by chemical bath deposition. We took as a reference the international guideline ISO 22036 for the determination of trace element mass fraction in geological samples (extracts of soil) by ICP-AES [21]. The method was validated according to AFNOR Norm NFT 90-210 (2009) [22]. Estimation of an measurement uncertainty budget was carried out using a full combined measurement uncertainty calculation including possible sources of uncertainty according to EURACHEM and GUM guides [23,24].

Experimental

Preparation of Bismuth Sulfide Thin Films

Bismuth sulfide thin films were prepared by chemical bath deposition as reported in previous work [25]. Bismuth nitrate pentahydrate (Bi $(NO_3)_3$.$5H_2O$) was added into concentrated triethanolamine ($N(CH_2CH_2OH)_3$). The mixture was stirred ultrasonically until dissolution. Double distilled water was then added to obtain 0.1 mol L^{-1} of a complexed Bi^{3+} ion solution. To this preparation was added a definite volume of 1 mol L^{-1} solution of thiourea (NH_2SNH_2) used as a sulfide ion source. The mixture was poured into a round-bottomed flask placed in a water bath. The reaction took place in a basic aqueous medium. The pH was around 9. Temperature and time deposition was varied. Glass micro slides (26 x 15 mm - 1 mm thick) were used as substrates and dipped vertically. They were cleaned by immersion in an aqua regia acid solution for 2 min then washed profusely with distilled water. Black thin films were obtained and ultimately washed with distilled water then dried at room temperature.

Reference Solution and Samples Preparation for ICP-AES Analysis

Mono-elemental solution of 1g L^{-1} ICP Standard Certipur® (Merck, Darmstadt, Germany) containing the analyzed element (Bi) was used for calibration. Samples were placed in a beaker with concentrated nitric acid (3 mL) (65%, Carlo Erba for analysis ISO) and concentrated hydrochloric acid (5 mL) (37%, Carlo Erba for analysis ISO). Vessel contents were digested on a hot plate inside the fume hood at 110° ± 10°C for 15 min to dissolve the films. After cooling, obtained solutions were diluted with ultrapure water in 100 mL volumetric flasks (Class A) including 10% v/v of concentrated hydrochloric acid. The concentration of the solution was measured with ICP-AES using external calibration. Glass substrates were weighed before and after the acid digestion step to

determine the formed layer mass. All digestion vessels were previously cleaned in a bath of 10% v/v nitric solution for 48 h and washed with bi-distilled water.

Instrumentation

Measurements were carried out using an inductively coupled plasma atomic emission spectrometer Ultima C (Jobin Yvon, Horiba). The operating conditions employed were 1000 W RF power, 13 L min^{-1} plasma flow, 2 L min^{-1} sheath gas flow, 0.02 L min^{-1} nebulizer flow, and 1.5 mL min^{-1} sample uptake rate. The radial view was used for bismuth determination and three replicates were used to measure the analytical signal. Delay time for washing between samples and signal measurement was set to 150 s. High-purity argon (99.995%) was used to sustain plasma as well as a carrier gas.

Results and Discussion

Selection of Emission Line

Emission intensity was measured using two different spectral emission lines (atomic and ionic lines). Greater intensity values indicated higher sensitivity for bismuth on the atomic line at 223.061 nm.

Validation of the Method

Linearity According to the Maximum Tolerated Deviation Approach

According to the NF T90-210 standard, there are two approaches in order to validate the linearity of the analysis method. The global statistical approach and the maximum acceptable deviation approach. For the last one, the basic principle is to verify that all the observed biases on each analyzed standard are acceptable at a level specified by the laboratory for each standard. The working standard solutions of Bi were used to construct the calibration curves and bias assessment, basing on the validation protocol of the Norm.

The linearity of an analytical method is its ability to elicit test results that are directly, or by a well-defined mathematical transformation, proportional to the analyte concentration in sample solutions within a given range [26]. Linearity was evaluated by determining the emission intensities of five known concentrations of bismuth standard solutions ranging from 0.2 to 2.0 mg L^{-1}. Each calibration solution was measured once per day for five days. Mean intensities responses recorded for Bi were plotted against concentration. The correlation coefficient for bismuth was found to be 0.9996 which indicated good linearity. As shown in figure 1, the calibration plot for the determination of bismuth was: $y = 48130.4\, x + 9773.5$.
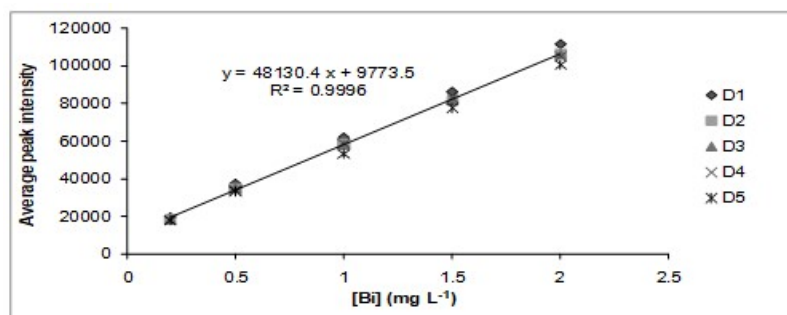

Figure 1: Linear calibration curve for the proposed procedure

Slopes and y-intercepts are estimated on each day of calibration. Each standard concentration is calculated and given in Table 1.

Day	Level 1	Level 2	Level 3	Level 4	Level 5
	0.2 mg L^{-1}	0.5 mg L^{-1}	1 mg L^{-1}	1.5 mg L^{-1}	2 mg L^{-1}
D1	0.17	0.53	1.01	1.49	1.99
D2	0.18	0.52	1.01	1.48	2.00
D3	0.18	0.53	1.00	1.50	2.00
D4	0.18	0.51	1.02	1.52	1.97
D5	0.19	0.53	0.97	1.50	2.01

Table 1: Obtained values of the standard solutions

Relative biases % corresponding to the difference between recovered values and theoretical calibration solutions were then calculated and represented according to a control chart (Figure 2). The calibration function was evaluated by fixing maximum tolerated deviations for each level of calibration solutions with 20 % for the lowest calibration concentration and 15% for the other ones.

The maximum tolerated deviation is determined based on the all-relative biases determination. It should be greater than the highest found value of the relative bias for the different concentration levels of the standard range. According to Standard NF T 90-210, the user sets a maximum acceptable deviation per calibration level consistent with the uncertainty due to the calibration that he wishes to accept in the next checks of the calibration ranges.
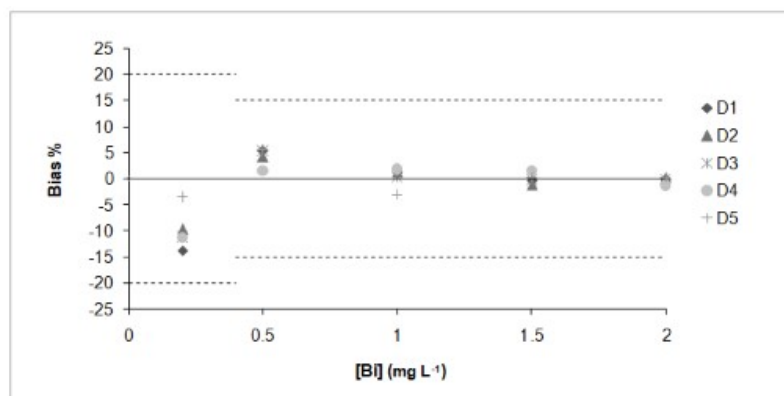

Figure 2: Relative biases % vs. true value of bismuth calibration solutions

Bias is a quantitative term describing the difference between the measured value of each standard concentration and its true value. In fact, testing linearity, it comes back to study the bias for acceptable accuracy and precision and this is through the verification of the absence of outliers and variances homogeneity for all the standard.

Relative biases have to be inferior to the maximum tolerated deviation fixed by the laboratory for each standard. As represented in the chart, results fulfill this criterion. Thus, the calibration function is considered acceptable in the studied range.

Study of the Presupposed Limit of Quantification

The limit of quantification (LOQ) of an analytical procedure is the lowest amount of analyte in a sample, which can be quantitatively determined with suitable precision and accuracy. It can be estimated using the following expression [27,28]:

$$y_{LOQ} = \bar{y}_{blank} + 10\, s_{blank} \qquad (2)$$

Where $\bar{y}_{\text{blank}}$ and s_{blank} are the average value of the blank signal and its corresponding standard deviation. LOQ value is 0.12 mg L-1. It is worth noting that the limit of detection (LOD) was also determined as 0.03 mg L-1 using equation (3).

$$y_{\text{LOD}} = \bar{y}_{\text{blank}} + 3\, s_{\text{blank}} \qquad (3)$$

Accuracy parameters estimation of the presupposed quantification limit was checked by analyzing ten repetitions (twice a day during five days) of a solution with a bismuth concentration of 0.1 mg L^{-1} to verify inequalities (4) and (5) (as shown in Table 2) [22].

$$\overline{z_{\text{LOQ}}} - 2 \times s_{\text{LQ}} > \text{LOQ} - 60\% \times \text{LOQ} \qquad (4)$$

$$\overline{z_{\text{LOQ}}} + 2 \times s_{\text{LOQ}} < \text{LOQ} + 60\% \times \text{LOQ} \qquad (5)$$

With, $\overline{z_{\text{LOQ}}}$ The overall average of the measured value, LOQ: The presupposed limit of quantification, and s_{LOQ}: The standard deviation.

Series number	5
Repetition number by series	2
General mean $\overline{z_{\text{LOQ}}}$ (mg L^{-1})	1.03 10^{-1}
The standard deviation of the intermediate precision s_{LOQ} (mg L^{-1})	3.08 10^{-3}
Relative standard deviation (%)	2.98
Presupposed limit of quantification: LOQ (mg L^{-1})	0.10
Maximum acceptable deviation: 60% × LOQ (mg L^{-1})	0.06
LOQ + 60% × LOQ (mg L^{-1})	0.16
$\overline{z_{\text{LOQ}}}$ + 2 × s_{LOQ} (mg L^{-1})	1.09 10^{-1}
$\overline{z_{\text{LOQ}}}$ -2 × s_{LOQ} (mg L^{-1})	9.7 10^{-2}
LOQ-60% × LOQ (mg L^{-1})	0.04

Table 2: Figures of merit of the presupposed limit of quantification

Both inequalities were confirmed. Therefore, the accuracy of the limit of quantification at 0.12 mg L^{-1} of bismuth is verified.

A recovery study of Matrix Effects

The method of standard additions was applied to investigate whether matrix effects exist through this proposed method. Known amounts of the targeted element were spiked to ten samples. Recovery of added contents is calculated using equation (6) and presented in Table 3:

$$\text{Recovery}(\%) = \frac{Found\ content - Initial\ content}{Added\ content} \qquad (6)$$

Samples	Initial content(mg L^{-1})	Content of Bi added(mg L^{-1})	Content of Bi found(mg L^{-1})	Recovery(%)
1	0.2419	0.2	0.4387	98
2	0.2120	0.2	0.4094	99
3	0.3533	0.2	0.5700	108
4	0.4013	0.2	0.5916	95
5	0.2740	0.2	0.4760	101
6	0.4028	0.2	0.5958	96
7	0.4285	0.2	0.6197	96
8	0.3760	0.2	0.5837	104
9	0.3401	0.2	0.5215	91
10	0.3186	0.2	0.5091	95

Table 3: Recovery values

Initial contents were obtained following a dilution to be in the adequate range of calibration. Recovery values range from 91 to 109%. No recovery correction will be applied in the expression of the result, as the average recovery value is acceptable with respect to a maximum bias of 10% around 100% set by the laboratory in accordance with the level of concentration studied. The Horwitz ratio (HorRat) could have also been used as a reference to calculate the maximum bias from the Horwitz equation CV Horwitz (%) = $2 C^{(-0.15)}$, where C is the concentration found or added, expressed as a mass fraction. For example, for C= 0.2 mg/L, the maximum bias is 20 %, double what was set [22, 29]

Accuracy (Trueness and Precision)

the study of matrix effects according to the NF T90-210 standard shows the absence of any matrix effects on bismuth analysis. Therefore, accuracy study using standard solutions was considered valid.

The study of accuracy refers to the assessment of intermediate precision and bias against values that serve as references [22]. To verify the accuracy in our range of calibration, a certified reference material Certipur® 119804 (1000 ± 5 mg L^{-1} of Bi) was used to prepare a solution of certified material with a concentration of 1.00 ± 0.005 mg L^{-1}. It was prepared according to procedure and analyzed twice a day for five days. Results are given in Table 4.

Day	Repetition		Mean	Variance
	1	2		
D1	0.9977	1.0038	1.0007	1.85×10^{-5}
D2	1.0047	0.9960	1.0004	3.74×10^{-5}
D3	0.9979	0.9970	0.9974	3.55×10^{-7}
D4	1.0028	1.0046	1.0037	1.61×10^{-6}
D5	0.9963	1.0038	1.0000	2.81×10^{-5}

Table 4: Certified reference material measurements results (in mg/L)

Trueness and precision of the method are assessed by verifying inequalities (7), (8), and (9). Results are given in Table 5 and interpreted according to a maximum acceptable deviation (EMA) of 10 % set by the laboratory.

$$\overline{z_{\mathrm{Bi}}} + 2 \times s_{\mathrm{Bi}} < C_{\mathrm{CRM}} + \mathrm{EMA} \qquad (7)$$

$$\overline{z_{\mathrm{Bi}}} - 2 \times s_{\mathrm{Bi}} > C_{\mathrm{CRM}} - \mathrm{EMA} \qquad (8)$$

ND: the normalized deviation; $$\mathrm{ND} = \frac{\left|\overline{Z_{\mathrm{Bi}}} - C_{\mathrm{CRM}}\right|}{\sqrt{\dfrac{s_{\mathrm{Bi}}^2}{n} + u_{\mathrm{CRM}}^2}} < 2 \qquad (9)$$

Where,

- $\overline{Z_{\mathrm{Bi}}}$: The overall mean measured bismuth concentration,

- s_{Bi}: Standard deviation of the Intermediate precision,

- C_{CRM}: bismuth certified reference value,

- EMA: The maximum acceptable deviation fixed by the laboratory,

- u_{CRM} : Calculated uncertainty of the prepared certified reference material.

Series number	5
Repetition number by series	2
General average : $\overline{Z_{\mathrm{Bi}}}$ (mg L^{-1})	1.0005
The standard deviation of the Intermediate precision: s_{Bi}(mg L^{-1})	0.0041
Relative standard deviation (%)	0.41
Reference value: C_{CRM} (mg L^{-1})	1
C_{CRM} + EMA (mg L^{-1})	1.1
$\overline{Z_{\mathrm{Bi}}}$ +2×s_{Bi} (mg L^{-1})	1.0088
$\overline{Z_{\mathrm{Bi}}}$ -2×s_{Bi} (mg L^{-1})	0.9922
C_{CRM} – EMA (mg L^{-1})	0.9
u_{CRM} (mg L^{-1})	0.0025
ND (mg L^{-1})	0.02

Table 5: Figures of merit of the accuracy of the method

There is good agreement between measured and certified values. Inequalities (7) and (8) were confirmed. In addition, normalized deviation (ND) calculated according to the equation (9) was found to be inferior to 2 which is the upper warning for a level of confidence of 95 % (k=2) as recommended by AFNOR Norm NFT 90-210 (2009). Therefore, method trueness and accuracy for a certified reference value of 1.00 ± 0.005 mg L^{-1} of Bi are verified.

Estimation of Uncertainty of the Analytical Method

Uncertainty of the measurement result, e.g. of an analytical determination, is a parameter pertaining to a given measurement result and describing the spread of the values, which can be ascribed to the measured quantity[30-32].

The uncertainty assessment of bismuth analysis has been carried out based on the general approach for estimating measurement uncertainty (Application of the procedure described in the GUM, Chapter 8). The first step is to determine all the causes of uncertainty and the influencing factors, which can be performed using the 5M ((material, matter, means (human resources), medium (environment), method) chart given in the seven steps in Chapter 7. After that, calculating the measurement result Y, calculating standard uncertainties u (xi) propagation of uncertainty using the law of propagation of uncertainty and finally expressing the measurement result and its associated uncertainty.

Bismuth mass fraction was calculated from the following equation (10):

$$W_{\text{Bi}}\% = \frac{C_{\text{ICP}} \times V}{m_{\text{sample}}} \times D \times 100 \qquad (10)$$

Where; C_{ICP} is the bismuth concentration as read from the calibration curve (mg L^{-1}), V is the volume of the prepared solution, m_{sample} is the test portion mass (mg) and D is the dilution factor applied to the sample.

Uncertainty estimation was performed by specifying factors contributing to the measured analytical signal. Sources of uncertainty were identified and their influence on the final evaluated result. Their identification was based on a flowchart describing the measurement process (Figure.3) and a cause-and-effect diagram (Figure.4). Bismuth weight percentage was mainly affected by the following sources of uncertainty: calibration solutions preparation, calibration curve (C_{ICP}), the volume of the final solution to analyze (V), sample weight (m_{sample}), and accuracy of the method. The effect of temperature should also be considered, as it is reflected in liquid expansion and in volumetric deviations when preparing solutions. The influence of the conversion of the solid bismuth sulfide into the solution was not taken into consideration because on the one hand bismuth oxide is very soluble in acids and on the other hand the absence of incomplete digestion has been verified by finding the same quantities of Bi initially used to synthesize this oxide. Therefore, its quantification is difficult to estimate, and it is evaluated indirectly on the sample submitted for analysis. Sources of uncertainties with a negligible effect were not taken into consideration (arrows checked) such as the pressure, the humidity, and the ability of technical staff to conduct appropriately the analysis which was tested beforehand (Figure.4).
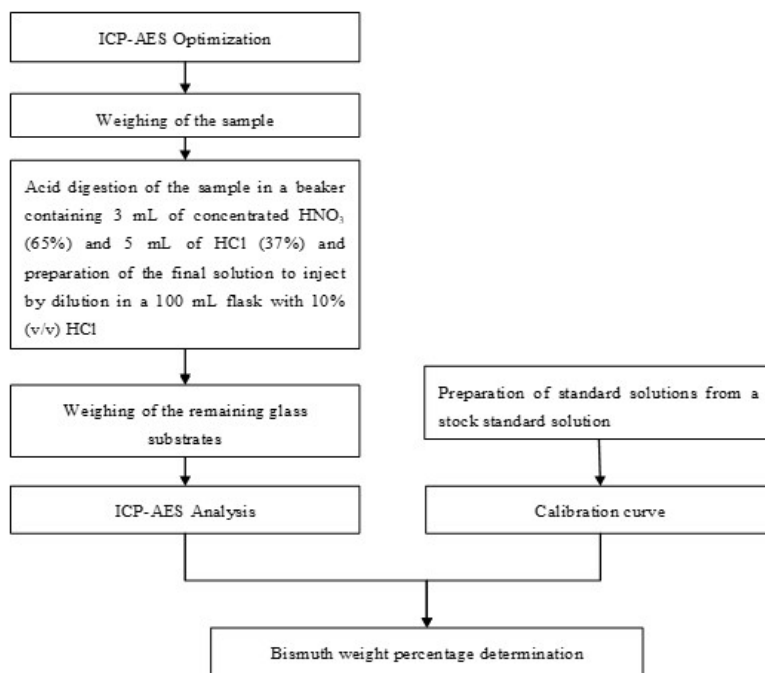
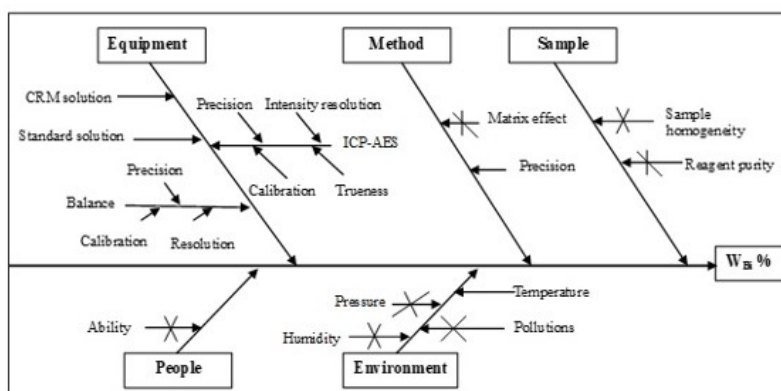**Figure 3:** Flowchart of bismuth analysis process by ICP-AES

Figure 4: Cause and effect diagram for the bismuth analysis by ICP-AES

Based on equation (10), combined uncertainty $u_c(W_{Bi})$ can be calculated according to equation (11). It takes into account standard uncertainties of all significant individual steps of the measurement process:

$$u_c(W_{Bi}) = W_{Bi} \times \sqrt{\left(\frac{u_c(C_{ICP})}{C_{ICP}}\right)^2 + \left(\frac{u_c(V)}{V}\right)^2 + \left(\frac{u_c(m)}{m}\right)^2 + \left(\frac{u_c(D)}{D}\right)^2}$$

(11)

Where: $u_c(C_{ICP})$: combined uncertainty derived from the concentration of the sample solution as read from the calibration curve,

$u_c(V)$: combined uncertainty arising from the flask volume,

$u_c(m)$: combined uncertainty derived from the test portion mass,

$u_c(D)$: combined uncertainty derived from the factor of dilution.

Combined Uncertainty Arising from the Flask Volume, Uc(V)

Uncertainty derived from the sample preparation is a combination of both uncertainties from the calibration of the flask volume u(Vcalibration) and temperature effect u(Teffect). The effect of the meniscus whose value is negligible compared to the other terms was not taken into account. These sources were combined in the following equation:

$$u_c(V) = \sqrt{u^2(\text{Vcalibration}) + u^2(\text{Teffect})} \qquad (12)$$

The uncertainty associated with volumetric glassware was calculated using equation (13) following a type B triangular uncertainty evaluation. The maximum permissible deviation of 100 mL volumetric flask provided by the manufacturer is 0.01 mL. The temperature effect, determined using equation (14), describes dispersion produced by a variation of liquid temperature, through a rectangular distribution [23].

$$u(\text{Vcalibration}) = \frac{\text{Flask(Maximum permissible deviation)}}{\sqrt{6}} \qquad (13)$$

Where Flask (Maximum permissible deviation) = 0.01 mL

$$u(\text{Teffect}) = \frac{V \times 2.1\text{x}10^{-4} \times (T - 20)}{\sqrt{3}} \qquad (14)$$

With V = 100 mL and T= 25°C.

Therefore combined uncertainty arising from the flask volume u_c(V) is:

$$u_c(V) = \sqrt{\left(\frac{0.01}{\sqrt{6}}\right)^2 + \left(\frac{0.105}{\sqrt{3}}\right)^2} = \sqrt{\left(4.08\ 10^{-3}\right)^2 + \left(6.06\ 10^{-2}\right)^2} = 6.08\ 10^{-2} ml$$

$$(15)$$

Combined Uncertainty Arising from he Sample Weight, U$_c$(M)

This is a combination of uncertainties associated with balance indication error specified in calibration certificate u (calibration balance), resolution u (resolution) and precision u (precision) measurements. This uncertainty is expressed by the following equation (16).

$$u_c(m) = \sqrt{u^2(calibration\ balance) + u^2(resolution) + u^2(precision)} \qquad (16)$$

Where: u (calibration balance): standard uncertainty from calibration certificate considered as a normal distribution using a coverage factor of k=2 [32];

$$u(\text{calibration balance}) = \frac{U(\text{certificate calibration balance})}{2} \qquad (17)$$

Where U (certificate calibration balance) = 4 10^{-4} g.

u(resolution)uread: the resolution of the balance is a measure of an instrument's ability to display the exact value of the measurand. The uncertainty is determined by dividing the reading unit by $2\sqrt{3}$when using a digital display such as an analytical balance [24]:

$$u(resolution) = \frac{\text{Resolution}}{2 \times \sqrt{3}} \qquad (18)$$

Where resolution = 10^{-4} g.

u(precision): standard uncertainty due to repeatability is normally evaluated as the relative standard deviation s_r of the balance readings for n=3 successive loadings of the same weight [30].

$$u(precision) = \frac{s_r}{\sqrt{n}} \qquad (19)$$

Therefore, combined uncertainty arising from the sample weight $u_c(m)$ is:

$$u_c(m) = \sqrt{\left(2\ 10^{-4}\right)^2 + \left(2.89\ 10^{-5}\right)^2 + \left(1.05\ 10^{-2}\right)^2} = 1.02\ 10^{-2}g \qquad (20)$$

Combined Uncertainty Derived from Bismuth Concentration (C_{ICP}), $U_c(C_{ICP}$)

The relative uncertainty of bismuth concentration (C_{ICP}) was obtained from inverse calibration dependence as given by equation (21):

$$C_{ICP}\left(mgL^{-1}\right) = \frac{I - b}{a} \qquad (21)$$

Where I denote the corresponding ICP-AES signal, b is the y-intercept and a is the slope of the calibration.

Measurement results should be corrected for all recognized significant systematic effects. Indeed, measuring instruments and systems are often adjusted or calibrated using measurement standards and reference materials to correct systematic effects. Uncertainties associated with these standard materials and correction must be taken into account [23]. Having inserted the extra effect standard solutions accuracy, method accuracy into the cause-and-effect diagram, the implied model for calculating C_{ICP} becomes:

$$C_{ICP}\left(mgL^{-1}\right) = \frac{I - b}{a} \times f_{\text{standard solution accuracy}} \times f_{\text{method trueness}} \times f_{\text{method precision}} \qquad (22)$$

Where faccuracy std sln, fmethod truness and fprecision f $_{standard\ solution\ accuracy}$f std sln accuracy, fmethod truness and fmethod precision , f $_{method\ trueness,}$ and f $_{method\ precision}$ are correction factors assumed to be unity in the original calculation and representing the effect of standard solutions, method trueness, and precision, respectively.

Assuming an additive model of uncertainty sources and insignificant pair-wise correlations, uncertainty $u_c(C_{ICP})$ can be calculated according to the following equation (23).

$$u_c(C_{\text{ICP}}) = \overline{C_{\text{ICP}}} \times \sqrt{\left(\frac{u(\text{I}-\text{b})}{\text{I}-\text{b}}\right)^2 + \left(\frac{u(a)}{a}\right)^2 + \sum_{i=1}^{n=5}\left(\frac{u(C_{\text{stdsol}(i)})}{C_{\text{stdsol}(i)}}\right)^2 + \left(\frac{u(\text{Trueness}_{\text{CRM}})}{C_{\text{CRM}}}\right)^2 + \left(\frac{u(\text{Precision}C_{\text{ICP}})}{\overline{C_{\text{ICP}}}}\right)^2}$$

(23)

Where:

- $\overline{C_{\text{ICP}}}$ is the mean value obtained from a series of measurements.

- I-b = a x C_{ICP} 　　　(24)

- Where; a and b are the slope and y-intercept from calibration curves.

- uncertainties u(I-b) and u(a) are experimentally determined by performing three calibration curves:

$$u(\text{I}-\text{b}) = \sqrt{u^2(I) + u^2(b)}$$ 　　(25)

Where $u(I) = \dfrac{\text{Intensity resolution}}{2 \times \sqrt{3}}$; Intensity resolution = 10^{-4} (u.a)　(26)

$$u(b) = \sqrt{\frac{\sum_{i=1}^{n}(b_i - \bar{b})^2}{n-1}}$$ 　　(27)

$$u(a) = \sqrt{\frac{\sum_{i=1}^{n}(a_i - \bar{a})^2}{n-1}}$$ 　　(28)

Where, $\bar{a}$ and $\bar{b}$ are the mean of all slopes and the y-intercepts from calibration curves. n is the total number of measurements.

- $u(C_{\text{std sol}(i)})$: is the uncertainty arising from the preparation of calibration solutions.

- Contributions of uncertainties are derived from the volumetric flask (V_f) and pipettes (Vp) used to prepare standard solutions. It is calculated as follows:

$$C_{\text{stdsol}(i)}\left(\text{mg}\,L^{-1}\right) = \frac{C_{\text{CRM}} \times V_{\text{p1}} \times V_{\text{p2}}}{V_{\text{f1}} \times V_{\text{f2}}}$$ 　　(29)

Application of propagation uncertainty law gives:

$$\left(\frac{u_c(C_{\text{stdsol}(i)})}{C_{\text{stdsol}(i)}}\right)^2 = \left(\frac{u(C_{\text{CRM}})}{C_{\text{CRM}}}\right)^2 + \left(\frac{u(V_{\text{p1}})}{V_{\text{p1}}}\right)^2 + \left(\frac{u(V_{\text{p2}})}{V_{\text{p2}}}\right)^2 + \left(\frac{u(V_{\text{f1}})}{V_{\text{f1}}}\right)^2 + \left(\frac{u(V_{\text{f2}})}{V_{\text{f2}}}\right)^2$$

(30)

Where:

$u(C_{std\ sol(i)})$: Concentration uncertainty of each standard calibration solution.

$C_{std\ sol(i)}$: Concentration of each standard calibration solution

$u(C_{CRM})$: Standard uncertainty of the certified reference material.

C_{CRM}: Concentration of the certified reference material.

$u(V_{P1})$: Standard uncertainty of the pipette volume used to prepare the intermediate solution.

V_{P1}: Volume taken from the CRM solution.

$u(V_{P2})$: Standard uncertainty of the pipette volume used to prepare the standard solution.

V_{P2}: Volume taken from the intermediate solution.

$u(V_{f1})$: Standard uncertainty of the flask volume of the intermediate solution.

V_{f1}: Volume of the intermediate solution flask.

$u(V_{f2})$: Standard uncertainty of the flask volume of the standard solution.

V_{f2}: Volume of the standard solution flask.

$u(\text{Trueness }_{CRM})$ is the uncertainty of method trueness determined based on the normalized deviation ND criteria given by equation (31):

$$\text{ND} = \frac{|\bar{x}_i - x_{\text{CRM}}|}{\sqrt{u_i^2 + u_{\text{CRM}}^2}} \qquad (31)$$

Where, $\bar{x}_i$, x_{CRM}, u_i, and u_{CRM} are mean value obtained from series of measurements, the value of certified reference material CRM, uncertainty from repeatability, and uncertainty of certified reference material provided by the supplier.

$$u_i = \frac{s_r}{\sqrt{n}} \qquad (32)$$

If the normalized deviation is inferior to 2:

$$u(\text{Trueness}_{\text{CRM}}) = \frac{U_{\text{CRM}}}{k} \qquad (33)$$

Where k=2 for a normal distribution.

- $u(\text{precision } C_{ICP})$: The uncertainty of repeatability of a real sample C_{ICP}, calculated as standard deviation (S.D) of n=3 readings on calibration curve.

$$u(\text{Precision C}_{\text{ICP}}) = \frac{s_r}{\sqrt{n}} \qquad (34)$$

The combined uncertainty derived from bismuth concentration $u_c(C_{ICP})$ is, therefore:

$$u_c(C_{ICP}) = 1.77 \times \sqrt{(2.93\ 10^{-3})^2 + (3.34\ 10^{-3})^2 + (8.62\ 10^{-3})^2 + (2.5\ 10^{-2})^2 + (6.18\ 10^{-3})^2} = 0.05\ mgL^{-1}$$

$$(35)$$

Combined Uncertainty Arising from the Factor of Dilution D, $U_c(D)$

A 10 fold dilution using a 10% (v/v) HCl solution was applied during the ICP –AES method to work in the adequate range of concentrations. Two contributions constitute the uncertainty arising from the dilution factor, the uncertainty about the pipette (V_{P3}) and the uncertainty from the final volumetric flask (V_{f3}).

$$u_c(D) = D \times \sqrt{\frac{u^2(VP3)}{VP3} + \frac{u^2(Vf3)}{Vf3}} \qquad (36)$$

Where VP3 = 10 mL the pipette volume which maximum permissible deviation is 0.05 mL. V_{f3} = 100 mL the final flask volume which maximum permissible deviation is equal to 0.01 mL. Their uncertainties are determined following equations (12), (13) and (14). The uncertainty associated with the factor of dilution is, therefore:

$$u_c(D) = 10 \times \sqrt{\frac{4.53\ 10^{-4}}{10} + \frac{3.69\ 10^{-3}}{100}} = 2.21\ 10^{-2} mL \qquad (37)$$

Expanded uncertainty is required to provide an interval that may be expected to encompass a large fraction of the distribution of values which could reasonably be attributed to the measurand [32]. Estimation of the expanded uncertainty (U) was calculated using a coverage factor k = 2, with a 95% confidence interval of the results obtained. For more clarity, all the values of the uncertainty components are summarized in Table 6.

$U = u_c(W_{Bi}) \times k$ (34)

Parameter	Value (X)	u(X)	u(X)/X
Sample weight (mg)	3.17	$1.05\ 10^{-2}$	$3.32\ 10^{-3}$
Flask volume (mL)	100	$6.08\ 10^{-2}$	$6.08\ 10^{-4}$
Bismuth concentration C_{ICP} (mg/L)	1.77	0.05	$2.75\ 10^{-2}$
Dilution factor	10	$2.21\ 10^{-2}$	$2.21\ 10^{-3}$
Bismuth mass fraction (%)	55.33		
combined standard uncertainty	1.54		
Expanded uncertainty (k=2) (%)	3.08		

Table 6: Calculation of the expanded uncertainty

Bismuth analysis by ICP-AES on thin films has not been reported up to date. This could be explained by the destructive nature of the analysis, unlike other techniques such as the Energy Dispersive X-ray (EDX) microanalysis. Therefore, comparison with experimental data from other sources is impractical. Results showed that major contribution to measurement uncertainty was derived from concentration determination by ICP-AES and thus from calibration solutions preparation, calibration, trueness, and

precision of the method. Contributions from the uncertainties associated with the sample weight, the final volume flask, and the dilution factor were insignificant.

Conclusion

This work addresses the issues regarding the use of an ICP-AES method which has been applied to estimate the Bi mass fraction of bismuth in bismuth sulfide thin films prepared by the chemical bath deposition method. This process has been validated in terms of linearity, the limit of quantification, selectivity, and accuracy. It was possible to identify the most significant uncertainties sources (CRM measurement and standard solution preparation wich was equal to $2.75 \ 10^{-2}$) and estimate the expanded uncertainty of the measurement (3.08%). The bismutn concentration determined by ICP-AES measurements was found to be equal to equal to 17.7 mg/L, representig 55.3% of the sample concentration wich is equal to 32 mg/L (3.2 mg of bismuth sulfide thin films dissolved in 100 ml of solution). the associated expanded uncertainty was found to be 3.08%. For this measurement example, the final result of bismuth determination can be expressed as follows (55.33%).

This study paves the way for the possible control of structural in addition to electrical and thermal conductivities of such films. Similarly, this research attempt will be able to extend to other works aimed at the recognition of metal traces in thin films based on sulfide compounds.

Conflict of Interest Statement

In addition, on behalf of all authors, I declare that there is no conflict of interest.

References

1. Yue Z, Wang X, Gu M (2018) Topological insulator materials for advanced optoelectronic devices.

2. Lan C, Luo J, Lan H, Fan B, Peng H et al. (2018) Enhanced Charge Extraction of Li-Doped TiO2 for Efficient Thermal-Evaporated Sb2S3 Thin Film Solar Cells. Materials 11: 355.

3. Tiwari KJ, Ren M-Q, Vajandar SK, Osipowicz T, Subrahmanyam A et al. (2018) Mechanochemical bulk synthesis and e-beam growth of thin films of Sb 2 Se 3 photovoltaic absorber. Sol Energy 160: 56-63.

4. Chao J, Xing S, Liu Z, Zhang X, Zhao Y et al. (2018) Large-scale synthesis of Bi2S3 nanorods and nanoflowers for flexible near-infrared laser detectors and visible light photodetectors. Materials Research Bulletin 98: 194-9.

5. Bhattacharya RN, Pramanik P (1982) Semiconductor Liquid Junction Solar Cell based on chemically deposited Bi2S3 thin Film and Some Semiconducting Properties of Bismuth Chalcogenides. J Electrochem Soc 129: 332-5.

6. Miller B, Heller A (1976) Semiconductor liquid junction solar cells based on anodic sulphide films. Nature 262: 680-1.

7. Konstantatos G, Levina L, Tang J, Sargent EH (2008) Sensitive Solution-Processed Bi2S3 Nanocrystalline Photodetectors. Nano Lett 8: 4002-6.

8. Desale DJ, Shaikh S, Siddiqui F, Birajdar R, Late R et al. (2013) Ghule A, Sharma R Enhancement of photosensitivity by annealing in Bi2S3 thin films grown using SILAR method. Composites, Part B 46: 1-6.

9. Jin R, Li G, Xu Y, Liu J, Chen G (2014) Uniform Bi2S3 nanorods-assembled hollow spheres with excellent electrochemical hydrogen storage abilities. Int J Hydrogen Energy 39: 356-65.

10. Cademartiri L, Scotognella F, O'Brien PG, Lotsch BV, Thomson J et al. (2009) Cross-linking Bi2S3 ultrathin nanowires: a platform for nanostructure formation and biomolecule detection. Nano Lett 9: 1482-6.

11. Yang X, Tian S, Li R, Wang W, Zhou S (2017) Use of single-crystalline Bi2S3 nanowires as room temperature ethanol sensor synthesized by hydrothermal approach. Sensors and Actuators 241: 210-6.

12. Yao K, Gong W, Hu Y, Liang X, Chen Q et al. (2008) Individual Bi2S3 nanowire-based room-temperature H2 sensor. The Journal of Physical Chemistry C 112: 8721-4.

13. Senila M, Drolc A, Pintar A, Senila L, Levei E (2014) Validation and measurement uncertainty evaluation of the ICP-OES method for the multi-elemental determination of essential and nonessential elements from medicinal plants and their aqueous extracts. J Anal Sci Technol 5: 37.

14. Momen AA, Zachariadis GA, Anthemidis AN, Stratis JA (2005) Development and Validation of Routine Analysis Methods for the Determination of Essential, Nonessential, and Toxic Minor and Trace Elements in Cereal and Cereal Flour Samples by Inductively Coupled Plasma–Atomic Emission Spectrometry. J AOAC Int. 88: 1797-810.

15. Tsygankova A, Makashova G, Shelpakova I, Saprykin A (2014) ICP-AES analysis of high purity bismuth oxide. Inorg Mater 50: 1397-401.

16. Carlini R, Carnasciali MM, Soggia F, Shen Y, Zanicchi G (2016) ICP-AES and microRaman corrosion behaviour investigation

on Pb, Sb, Bi tellurides in sodium chloride solution. J Alloys Compd 654: 593-8.

17. Dobrowolski R, Dobrzyńska J, Gawrońska B (2015) Determination of bismuth in environmental samples by slurry sampling graphite furnace atomic absorption spectrometry using combined chemical modifiers. Environ Monit Assess 187: 4125.

18. Schramel P, Xu LQ (1991) Determination of arsenic, antimony, bismuth, selenium and tin in biological and environmental samples by continuous flow hydride generation ICP-AES without gas-liquid separator. Fresenius' J Anal Chem 340: 41-7.

19. Moyano S, Gasquez J, Olsina R, Marchevsky E, Martinez L (1999) Pre-concentration system for bismuth determination in urine using FI-ICP-AES with ultrasonic nebulization. J Anal at Spectrom 14: 259-62.

20. P C Rao G, M Rao M, S Veni S, Seshaiah K, Ramesh A et al. (2006) Determination of bismuth in natural water samples by ICP-AES after preconcentration on dithiocarbamates-coated amberlite XAD-7. International Journal of Environmental Analytical Chemistry 86: 443-52.

21. ISO (2008) 22036 Soil quality - Determination of trace elements in extracts of soil by inductively coupled plasma - atomic emission spectrometry (ICP - AES).

22. AFNOR NFT90-210 (2009) Water quality- Protocol for the initial method performance assessment in a laboratory.

23. Ellison S L R, Williams A (2012) (Eds) Eurachem/CITAC guide: Quantifying Uncertainty in Analytical Measurement Third edition.

24. AFNOR NF ENV 13005 (1999) Guide pour l´expression de l´incertitude de mesure (GUM) (Guide to the expression of measurement uncertainty)

25. Dachraoui O, Merino JM, Mami A, León M, Caballero R et al. (2018) Annealing study and thermal investigation on bismuth sulfide thin films prepared by chemical bath deposition in basic medium. Appl Phys A. 124: 166.

26. ICH (1995) draft Guidelines on Validation of Analytical Procedures Definitions and terminology. Federal Register 60: 1126.

27. ISO/TS (2009) 13530, Qualité de l'eau - Lignes directrices pour le contrôle de qualité analytique pour l'analyse chimique et physicochimique de l'eau (Water quality - Guidelines for analytical quality control for chemical and physico-chemical analysis of water).

28. Eurachem (1998)-Guide The fitness for purpose of analytical methods -A laboratory guide to method validation and related Topics.

29. BIPM I, IFCC, ISO, IUPAC, IUPAP et al. (1993) International vocabulary of basic and general terms in metrology.

30. ISO (2012) 11352 Water quality - Estimation of measurement uncertainty based on validation and quality control data.

31. Dachraoui M (2016) Evaluation de l'incertitude des méthodes d'analyses chimique: méthodes analytiques du GUM et nouvelles approches de la norme ISO 11352. Centre de publication universitaire, Tunisia.